JCI insight

Pharmacogenomics of aromatase inhibitors in postmenopausal breast cancer and additional mechanisms of anastrozole action

Junmei Cairns, … , Mehrab Ghanat Bari, Liewei Wang

JCI Insight. 2020. https://doi.org/10.1172/jci.insight.137571.

Research In-Press Preview Oncology Therapeutics

Graphical abstract

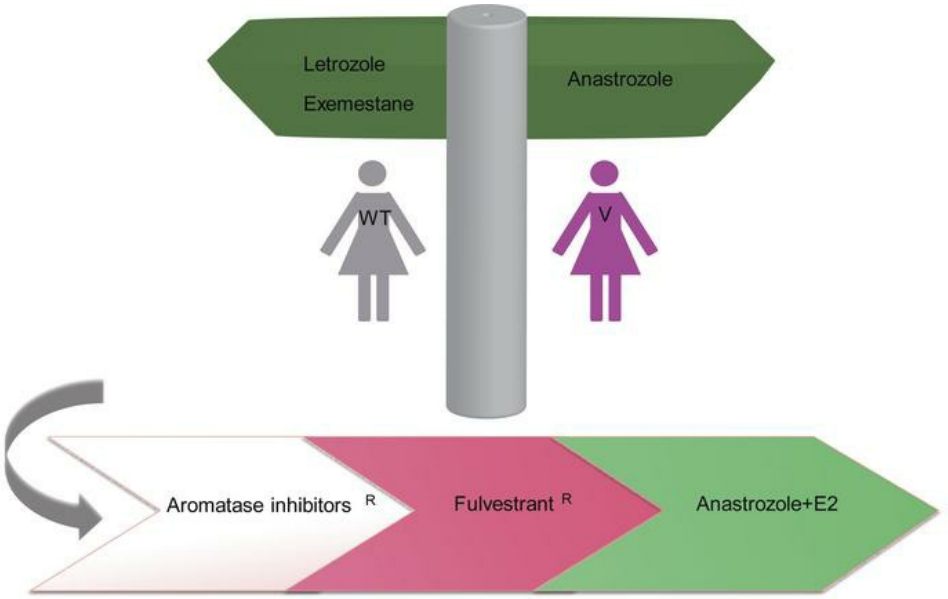

Pharmacogenomics of aromatase inhibitors in postmenopausal breast cancer and additional mechanisms of anastrozole action

Junmei Cairns[1], James N. Ingle [2], Tanda M. Dudenkov[1], Krishna R. Kalari[3], Erin E. Carlson[3], Jie Na[3], Aman U. Buzdar[4], Mark E. Robson[5], Matthew J. Ellis[6], Paul E. Goss[7], Lois E. Shepherd[8], Barbara Goodnature[9], Matthew P. Goetz[2], Richard M. Weinshilboum[1], Hu Li[1], Mehrab Ghanat Bari[1], Liewei Wang [1#]

Authors' Affiliations: [1] Department of Molecular Pharmacology and Experimental Therapeutics, Mayo Clinic, Rochester, MN USA; [2] Division of Medical Oncology, Mayo Clinic, Rochester, MN USA; [3] Department of Health Sciences Research, Mayo Clinic, Rochester, MN USA; [4] The University of Texas MD Anderson Cancer Center, Houston, TX USA; [5] Memorial Sloan Kettering Cancer Center, New York, NY USA;[6] Baylor Cancer Center, Houston, TX USA;[7] Massachusetts General Hospital, Boston, MA USA;[8] NCIC Clinical Trials Group, Kingston, Ontario, Canada;[9] Patient advocate, Mayo Clinic Breast Cancer Specialized Program of Research Excellence, Rochester, MN USA.

#Corresponding author: Liewei Wang, M.D., Ph.D., Mayo Clinic, 200 First Street S.W., Rochester, MN 55905, Email: wang.liewei@mayo.edu, phone: 507-284-5264; fax: 507-284-4455.

Conflict of interest statement: M.E.R reports honoraria from AstraZeneca; consulting or advisory from AstraZeneca (uncompensated), Change Healthcare, Daiichi-Sankyo (uncompensated), Epic Sciences (uncompensated), Merck (uncompensated), Pfizer (uncompensated); research funding from AbbVie (institution), AstraZeneca (Institution), Invitae (Institution, in-kind), Merck (Institution), Pfizer (institution), Tesaro (institution); travel, accommodation expenses from AstraZeneca, Merck; other transfer of value from AstraZeneca (editorial services), Pfizer (editorial services). M.J.E. reports employment with Bioclassifier, LLC; royalty income from Prosigma/Nanostring; honoraria from Nanostring, Novartis, AstraZeneca, Pfizer, Sermonix, Abbvie; patent interest from Bioclassifier, LLC, Prosigma/PAM50; P.E.G. reports research funding from Amgen; M.P.G. reports consulting roles with Lilly, Bovica, Novartis, Sermonix, Context Pharmaceuticals, and Genomic Health; R.M.W.

and L.W. are co-founders of, and stockholders in OneOme, LLC. All other authors have declared that they have no potential conflicts of interest.

Abstract

Aromatase inhibitors (AIs) reduce breast cancer recurrence and prolong survival, but up to 30% of patients exhibit recurrence. Using a genome-wide association study of patients entered on MA.27, a phase III randomized trial of anastrozole vs exemestane, we identified a SNP in CUB And Sushi Multiple Domains 1 (*CSMD1)* associated with breast cancer free interval, with the variant allele associated with fewer distant recurrences. Mechanistically, CSMD1 regulates *CYP19* expression in a SNP-, and drug-dependent fashion and this regulation is different among three AIs, anastrozole, exemestane, and letrozole. Overexpression of CSMD1 sensitized AI-resistant cells to anastrozole but not to the other two AIs. The SNP in CSMD1 that was associated with increased CSMD1 and CYP19 expression levels increased anastrozole sensitivity, but not letrozole or exemestane sensitivity. Anastrozole degrades estrogen receptor α (ERα), especially in the presence of estradiol (E2). ER positive breast cancer organoids and AI- or fulvestrant-resistant breast cancer cells were more sensitive to anastrozole plus E2 than to AI alone. Our findings suggest that the *CSMD1* SNP might help to predict AI response and anastrozole plus E2 serves as a potential new therapeutic strategy for patients with AI- or fulvestrant-resistant breast cancers.

Introduction

About 70% of primary breast cancers express estrogen receptor α (ERα). Adjuvant endocrine therapy, including aromatase inhibitors (AIs), is a standard treatment for these patients regardless of tumor size or nodal status. For postmenopausal women with primary ER-positive breast cancer, AIs are the standard-of-care to prevent relapse and prolong survival (1, 2). In advanced disease, AI-based therapy is a standard initial treatment. Despite their efficacy, about 19% of patients with early-stage disease suffer a recurrence by 10 years (1), and resistance to AIs in advanced or metastatic tumors invariably occurs (3). Therefore, there is a great need to understand the underlying mechanisms associated with AI response and resistance.

There are well accepted biomarkers associated with both *de novo* and acquired resistance to endocrine therapy (4, 5) and both host (germline) and somatic (tumor) alterations are known to contribute to resistance (6, 7). For example, the tumor genome has revealed several mechanisms of acquired AI resistance (8-10) such as amplifications or mutations that can activate ESR1 (10), and ligand -independent ERα activation of downstream pathways such as the phosphatidylinositol 3 kinase (11). At the same time, germline single nucleotide polymorphisms (SNPs) in *CYP19A1* have been associated with variation in circulating estrogen concentrations and with breast cancer risk (12).

In postmenopausal women, estrogen is mainly synthesized in peripheral tissues through the action of aromatase (CYP19A1). The main substrates, testosterone and androstenedione are transformed by aromatase into 17β-estradiol (E2) and estrone (E1), respectively. AIs potently inhibit aromatase and decrease estrogen levels. Two classes of AIs are currently in clinical use: steroidal, e.g. exemestane, which binds aromatase irreversibly, and non-steroidal, e.g. anastrozole and letrozole, which block the enzyme reversibly (13). While high body mass index (BMI) has been associated with AI resistance relative to tamoxifen (14, 15), suggesting variability in estrogen suppression might be associated with clinical outcome, and there are no biomarkers unique to an individual AI. Large phase III adjuvant clinical trials do not indicate any difference in efficacy between the three AIs (16, 17).

In the present work, following our previous observation that suppression of estrogens is associated with anastrozole treatment outcomes (18), we performed genome-wide association studies (GWAS) using changes in estrogen levels (before and after anastrozole) as the phenotype of interest using patients prospectively enrolled in the Mayo/M.D. Anderson/Memorial Sloan Kettering (designated M3) pharmacogenomics study (19). Here, we identified a series of SNPs that met genome-wide significance. To further determine whether these SNPs in genes associated with estrogen suppression were also associated with long term clinical outcome, we identified all SNPs within these gene regions based on the 1000 Genome Project and then examined their associations with breast cancer outcomes using GWAS data (7) previously obtained from the Canadian Cancer Trials Group MA.27 trial (16). MA.27 was a phase III trial comparing adjuvant anastrozole and exemestane treatment of post-menopausal women with ER positive breast cancer. The GWAS from the M3 clinical study identified SNPs within the human

CUB and Sushi multiple domains 1 (*CSMD1*) gene associated with changes in estrogen levels during anastrozole therapy. An additional SNP in *CSMD1* was also found to be associated with breast cancer free interval (BCFI) in MA.27. The variant SNP genotype was associated with longer BCFI. Functional studies indicated that the SNP altered the CYP19A1 expression in anastrozole-dependent fashion through transcription regulation. These findings further confirmed our previous observation (18) that anastrozole is different from exemestane and letrozole. Our previous study has already shown that anastrozole, but not letrozole or exemestane, acts as ERα ligand and degrader, and, in the current study, we further showed that the addition of E2 could sensitize cells to anastrozole, even in anastrozole- or fulvestrant-resistant models.

Results

GWAS of changes in estrogen levels and BCFI GWAS

To identify SNPs associated with AI estrogen suppression, we performed GWAS for changes in estrogen levels pre and post anastrozole in 624 postmenopausal women with resected early-stage ER positive breast cancer accrued through the M3 study (19). The flow diagram (Supplemental Figure 1A) shows the number of patients included in the analysis. We performed three GWA studies for changes in E1, E2, and the sum of E1 and E2 (Figure 1A and Supplemental Figure 1B). Common SNPs reaching genome wide significance ($p<5E-08$) among the three GWAS included rs2449598 within *DLG2* on chromosome 11 ($p=2.23E-10 \sim 1.24E-08$), rs1437153 near *CDH11* on chromosome 16 ($p= 2.82E-9 \sim 2.7E-8$), and rs6981827 in the intron of the *CSMD1* gene on chromosome 8 ($p=2.02E-8 \sim 2.12E-8$) (Figure 1A; Supplemental Figure 1B; Supplemental Table 1). The variant alleles for these SNPs were associated with less estrogen suppression during AI treatment.

Because M3 was a pharmacokinetic and pharmacodynamic study, outcome data were not available and we examined the SNPs identified in M3 in the MA.27 trial where we had long-term follow-up (16). We identified all SNPs in *DLG2, CDH11,* and *CSMD1* gene regions (100 kb up and down stream of the gene) using data from the 1000 Genome Project and determined their association with BCFI in MA.27 for which GWAS results were available (7). The most

significant association with the MA.27 BCFI phenotype was the rs6990851 SNP in the *CSMD1* gene (p=4.83E-06, HR=0.56) (Figure 1B). The variant allele (MAF=0.21) for rs6990851 was associated with longer BCFI (Figure 1C). No difference was observed between the two drugs with regard to SNP effect on BCFI. The rs6990851 SNP from MA.27 and the rs6981827 from M3 were only weakly linked in the M3 breast cancer patients ($r^2 = 0.014$) and the MA.27 population ($r^2 = 0.02$). Therefore, neither of the SNPs was significantly associated with the other phenotype. The *CSMD1* variant SNP, rs6981827 (MAF=0.05), associated with less estrogen change in the M3 study (effect size= -0.60), was not an eQTL SNP for *CSMD1* gene expression based on GTEx, while the *CSMD1* SNP rs6990851, which was associated with longer BCFI was associated with higher *CSMD1* expression level in adipose and brain tissues, and with a trend in breast tissue (Supplemental Figure 1C).

Rs6990851 showed SNP- and anastrozole- dependent transcriptional regulation of CSMD1 and CYP19A1

We first determined whether the expression of *CSMD1* might be estrogen-dependent. We treated ER-expressing ZR75-1 and T47D cells with 0.1 nM E2 and observed that *CSMD1* mRNA was significantly induced ($p < 0.01$; Supplemental Figure 2). Because the known mechanism of action of AIs is to block aromatase activity, we then tested a possible relationship between the expression of CSMD1 and CYP19A1. Overexpression of CSMD1 increased CYP19A1 expression levels in breast cancer cells and human adipocytes (Figure 2A). We then used ENCODE data to search for putative estrogen response elements (EREs) and identified two EREs within 500 bp of the *CSMD1* SNP, rs6990851. Rs6990851 mapped to intron 1 of *CSMD1* and two EREs were detected at 291 bp upstream and 296 bp downstream, respectively, while rs6981827 did not have any EREs within 500bp, in addition to its lack of eQTL relationship with *CSMD1*. Therefore, we focused on rs6990851 for further functional studies. Based on our prior experience of studying SNP effects on gene expression and hormonal therapy, we took advantage of cell lines selected on the basis of *CSMD1*genotype from a genomic data-rich panel of lymphoblastoid cell lines (LCLs) that has already proven to be a powerful tool for generating and testing pharmacogenomic hypotheses (20) (21). We first exposed LCLs selected based on the rs6990851 SNP genotype to hormones or AIs to determine the effect of the SNP on *CSMD1* and *CYP19A1* expression. This is a strategy that we commonly used to determine the functional

impact of GWAS signals (7, 20). LCLs with homozygous WT or variant genotypes for the *CSMD1* rs6990851 SNP were treated with increasing concentrations of androstenedione, a precursor of estrogen and *CSMD1* and *CYP19A1* mRNA levels were determined. Cells with homozygous WT SNP genotype showed increased expression of *CSMD1* and, in parallel, *CYP19A1* expression (Figure 2B-D). In contrast, in LCLs with the variant allele, *CSMD1* and *CYP19A1* expression was virtually unchanged with androstenedione. Importantly, addition of anastrozole reversed the expression patterns of *CSMD1* and *CYP19A1* (Figure 2B). Specifically, addition of anastrozole increased *CSMD1* and *CYP19A1* expression in cells with the variant SNP genotype, but decreased *CSMD1* and *CYP19A1* levels to or below baseline in cells with the WT allele (Figure 2B and E). Interestingly, neither letrozole nor exemestane (Figure 2C-D) significantly changed the expression patterns of *CSMD1* and *CYP19A1* comparing between WT and variant LCLs.

To determine whether the SNP impact on gene expression reflects differential binding of ERα to EREs that are located in close proximity of rs6990851, we performed ChIP assays using an ERα antibody. We found that the rs6990851 SNP effect occurred through the ERE that located 296 bp upstream from the SNP (Figure 2F) and resulted in an increased binding of ERα in WT cells treated with androstenedione, A similar result was observed in variant cells when anastrozole was added (Figure 2G, left panel). However, no differential binding to the second ERE located 291 bp downstream from the SNP was detected (Supplemental Figure 3). Furthermore, we did not observe any SNP-dependent binding with letrozole or exemestane (Figure 2G, right panel).

Rs6990851 alters anastrozole response through CSMD1 and CYP19A1

We next sought to determine the functional consequences of the *CSMD1* SNP on response to AIs. LCLs homozygous for the variant SNP, which resulted in high CSMD1 expression, were more sensitive to anastrozole than homozygous WT or heterozygous LCLs (Figure 3A, left panel), whereas these different alleles had little effect on letrozole or exemestane sensitivity (Figure 3A, middle and right panel). To assess the role of *CSMD1* in AI response in breast cancer cells, we used the MCF7/AC1 cell line because of its high expression of the AI target, CYP19A1. Additionally, LetR (22), a letrozole resistant cell line, was used to determine the role of *CSMD1* in AI response in an AI-resistant setting. Finally, we also used human adipocytes because adipose tissue is the predominant source of estrogens in post-menopause women (23). In

all three lines, overexpression of CSMD1 significantly increased anastrozole sensitivity compared to empty vector, whereas overexpression of CSMD1 showed little effect on letrozole and exemestane sensitivity (Figure 3B). These findings were also observed in two other ER-positive breast cancer cell lines (T47D, ZR75-1) (Supplemental Figure 4). To further define the relationship between CSMD1 and CYP19A1, we attempted to reverse the AI sensitization effect resulting from CSMD1 overexpression by knocking-out endogenous *CYP19A1* using CRISPR/Cas9 methodology in T47D cells (Figure 3C). As shown in Figure 3D, *CYP19* knockout abrogated the effect of CSMD1 overexpression on survival, indicating that *CYP19* is a major target that mediates the effect of *CSMD1* on anastrozole response. CSMD1 was recently shown to interact with SMAD3 in melanoma cells (24). SMAD3, activated by TGFβ3, was required for steroidogenic Factor-1 (SF-1) binding to the *CYP19A1* type II promoter (25). We, therefore, investigated whether CSMD1 might be a component of the SMAD3– TGFβ3 receptor (TGFβR) complex involved in *CYP19A1* transcription regulation. CSMD1 co-precipitated SMAD3 in breast cancer cells and human adipocytes, and a reciprocal immunoprecipitation further confirmed the interaction (Figure 3E). Overexpression of CSMD1 enhanced the interaction between SMAD3 and TGFβR and resulted in SMAD3 activation as evidenced by increased pSMAD3 (Figure 3F). This regulation of *CSMD1* on *CYP19A1* was impaired after the knockdown of *SF-1* or *SMAD3* (Supplemental Figure 5). These results suggest that CSMD1 is a scaffolding protein that brings SMAD3 and TGFβR together and promotes phosphorylation of SMAD3. To further confirm that the regulation of the *CSMD1* SNP on AI response is through CSMD1/SMAD3/CYP19A1 axis, we treated LCLs carrying either WT or variant SNP genotypes with androstenedione alone or in combination with an individual AI. As shown in Figure 3G, cells with different rs6990851 SNP genotypes showed striking differences in pSMAD3 and CYP19A1 levels. In particular, WT cells had increased pSMAD3 and CYP19A1 levels after androstenedione treatment, and significantly reduced pSMAD3 and CYP19A1 levels when anastrozole was added. Importantly, addition of letrozole or exemestane did not alter the protein levels in WT cells. In contrast, in the variant cells, androstenedione treatment did not change pSMAD3 and CYP19A1 levels compared to vehicle treatment, while addition of anastrozole, but not letrozole or exemestane, significantly upregulated pSMAD3 and CYP19A1 levels. Therefore, rs6990851 upregulated CSMD1 expression in the presence of anastrozole, but not the

other two AIs (Figure 2), resulting in SMAD3 activation and increased *CYP19A1* gene expression (Figure 3G), leading to increased sensitivity to anastrozole (Figure 3A).

Anastrozole potentiates estrogen effect on ERα transcription activity and ERα degradation

The observation of the *CSMD1* SNP and AI-dependent regulation of gene expression and differential response to individual AI further confirmed our previous finding. Our previous studies indicated that anastrozole is different from the other two AIs by possessing a second mechanism of action (18), being an ERα agonist in a similar fashion to E2. It can activate ERα-dependent transcription, but the effect decreased with increasing concentrations of anastrozole due to induction of ERα degradation (18). To further explore the impact of anastrozole effect on ERα activation and degradation, we tested various concentrations of E2 and anastrozole as well the two combined. We showed that anastrozole plus E2 at 0.1 or 1 nM showed ~2.4- and 3.01-fold increase in luciferase activity compared to anastrozole or E2 alone at that concentration in *CYP19* knock out (KO) T47D cells (Figure 4A, $p < 0.001$). However, when E2 concentration increased to 10 nM, combination with anastrozole led to a significant inhibition in luciferase activity compared to anastrozole or E2 alone (Figure 4A, $p < 0.001$). Letrozole and exemestane had no impact on E2 induced luciferase activity (Figure 4A). These observations suggest that anastrozole has a cumulative effect with low dose E2 to activate ERα mediated transcriptional activation. While at higher concentration of E2, it showed a cumulative effect with anastrozole on ERα degradation, leading to reduced ERE dependent transcription activity. We further tested the combinaition effect on ERα protein level. Anastrozole (10 nM) combined with E2 at 10 or 100 nM decreased ERα protein level, while E2 or anastrozole at 10 nM alone was not able to degrade ERα (Figure 4B). Consistent with previous findings (26) showing that high concentrations of E2 led to a proteasome mediated degradation of ERα protein, we found that the proteasome inhibitor MG132, but not the autophagy inhibitor, 3MA, could inhibit the protein degradation induced by anastrozole (Figure 4C).

Anastrozole regulates a transcriptome distinct from E2 in breast cancer cells

Since anastrozole can function as an ERα ligand, to investigate whether anastrozole regulates similar or different sets of genes compared with E2, we performed RNA-seq using T47D breast cancer cells treated with anastrozole (10 nM) alone, E2 (0.1 nM) alone or anastrozole (10 nM)

+E2 (0.1 nM). These concentrations were chosen based on ability of anastrozole to increase luciferase activity without degrading ERα. Anastrozole alone significantly altered levels of 476 transcripts compared to the vehicle control (FDR <0.05), among which, 398 genes overlapped with E2 single treatment. As shown in the Venn diagram, anastrozole+E2 treatment resulted in altered expression of 513 transcripts, 204 of which were common with anastrozole alone, and 384 of the 513 were common with E2 alone treatment (Figure 4D, Supplemental Table 2, Supplemental Figure 6A). Selected genes identified by RNA-seq were further validated by qRT-PCR following anastrozole, E2 or anastrozole + E2 treatment (Supplemental Figure 6B). GSEA analysis for anastrozole treatment showed that compared with E2, anastrozole regulated genes involved in steroid biosynthesis, DNA replication, toxoplasmosis, VEGF signaling pathway, and actin cytoskeleton (Supplemental Table 3). Collectively, these findings suggest that, although at large, anastrozole behaves very similar to E2 with regard to its effect on downstream gene regulation (384 genes), and it also preferentially regulates pathways (204 genes) that are different from E2.

Therapeutic effect of the combination of anastrozole with E2

To test whether the combined effects of anastrozole and E2 on ERα protein degradation might lead to augmented anti-tumor activity compared with anastrozole alone, we evaluated cytotoxicity in *CYP19* KO, letrozole-resistant AC1-LetR and anastrozole-resistant MCF7/Ana^R cells (27) with anastrozole+/-E2 treatment. As shown in Figure 5A-C, 10 and 100 nM of E2 sensitized these cells to anastrozole, but not letrozole or exemestane, and anastrozole+10 nM E2 showed better therapeutic effect than any of the three AI alone in anastrozole resistant cells (Supplemental Figure 6C). Treatment with 10 or 100 nM E2 + 100 nM anastrozole also increased the degradation of ERα protein compared to cells exposed to 100 nM anastrozole alone (Figure 5D). It is important to emphasize that E2 alone, at the concentrations of 10 or 100 nM did not induce ERα degradation (Figure 5D), neither did it exert cytotoxic effect (Supplemental Figure 6D). To further confirm the combination effect, we used organoids grown from two primary ER positive breast cancer patients derived xenografts (PDXs) (28) and treated with anastrozole + E2. In all three organoids derived from two unique breast cancer patients, we confirmed ERα positivity (Figure 5E, Western blot). The dose response after 72h exposure to AI alone or in combination with 100 nM E2 was obtained. The number of survival organoids was

significantly reduced 72 h after exposure to anastrozole + E2, but not to letrozole or exemestane + E2 (Figure 5E). To further assess the drug combination effects over time (9 days), we used a luminescence survival assay. Here we selected a 200 nM anastrozole concentration based on the previous organoid response curves (Figure 5E). As shown in Figure 5F, anastrozole and E2 significantly inhibited organoid growth compared to anastrozole alone ($p < 0.01$).

Compared with the third-generation AIs, fulvestrant has superior efficacy and is a preferred treatment option for patients with hormone receptor-positive locally advanced or metastatic breast cancer based on the FALCON trial (29) and in the neoadjuvant setting based on the CARMINA 02 trial (30, 31). However, up to half of ER-positive metastatic breast cancer patients show intrinsic resistance, and ultimately all of them develop acquired resistance to fulvestrant (29). To test the efficacy of anastrozole plus E2 in the fulvestrant-resistant setting, we treated fulvestrant-resistant MCF7/164R-7 cells (27) with individual AI alone or combined with increasing concentrations of E2. We found that in fulvestrant-resistant cells, individual AI alone had a slightly better cytotoxic effect than fulvestrant. However, only anastrozole showed an E2 dose-dependent sensitization and this phenomenon was not observed for letrozole or exemestane (Figure 6A and Supplemental Figure 6E). Since fulvestrant is used in the AI-resistant setting, we then compared the response of anastrozole + E2 to fulvestrant in MCF7/Ana^{R}-2 cells. Our data revealed that the combination of anastrozole with 100 nM E2 showed an effect similar to that of fulvestrant (Figure 6B, top panel). MCF7/Ana^{R}-2 cell growth was dramatically reduced in the presence of 100 nM anastrozole + E2 after 3 days (Figure 6B, bottom panel). Even in endocrine-naïve breast cancer cells (MCF7AC1, ZR-75-1 and T47D), anastrozole plus E2 improved the therapeutic effects compared to anastrozole or fulvestrant alone (Figure 6B, top panel) (Figure 6B, bottom panel). Finally, anastrozole + E2 improved the therapeutic response in breast cancer PDXs organoids compared to fulvestrant (Figure 6C). Our findings suggest that anastrozole + E2 could improve outcome in both endocrine naïve and resistant breast cancers.

Discussion

This study has identified novel common genetic variants associated with estrogen suppression and breast cancer events in women treated with adjuvant AI therapy. None of these SNPs had

been previously reported in association studies (7, 12, 32). Our results not only help identify potential new biomarkers for the selection of patients who might benefit from AIs therapy, but also enhance our understanding of mechanisms involved in anastrozole action, all of which have significant clinical implications. For our GWAS, we used two independent studies with two different but related AI response phenotypes, estrogen suppression and BCFI, and we identified two SNPs in the *CSMD1* gene that were associated with one of these two phenotypes (Figure 1B-C). However, only rs6990851, but not rs6981827, was eQTL for *CSMD1*. These two SNPs have very low linkage disequilibrium. Previous studies have provided evidence that biochemical and genetic manipulations of motif-adjacent sequences can influence transcription factor activity (20, 33). Here we show that *CSMD1* regulation is estrogen dependent, and only the rs6990851 SNP dependent, but not the rs6981827 SNP. The rs6990851 SNP is in a region that has EREs within 500 bp of the SNP. We demonstrated that the rs6990851 SNP modifies ERα binding to an ERE in the *CSMD1* gene, leading to altered *CSMD1* and *CYP19* expression in an anastrozole-dependent fashion (Figure 2G). Mechanistically, CSMD1 regulated *CYP19A1* gene transcription by acting as a scaffolding protein for SMAD3 and TGFβR (Figure 3E-G and Supplemental Figure 5). The variant rs6990851 SNP allele that increased *CSMD1* expression also increased sensitivity to anastrozole, but not letrozole or exemestane (Figure 3). This result strongly suggested potential differences in mechanisms of action between anastrozole and the other two AIs, which was also confirmed in our previous finding (18). We did not observe a SNP-drug interaction in the MA.27 trial and the SNP showed a protective effect regardless of the treatment arm, exemestane vs. anastrozole. Based on the SNP-dependent drug effects on *CSMD1* and *CYP19* in LCLs, we concluded that the variant rs6990851 SNP results in lower expression of *CSMD1* and, in turn *CYP19*, in the presence of androstenedione, leading to slow cell proliferation and better prognosis. The addition of exemestane or letrozole did not change the *CSMD1* and *CYP19* expression patterns compared to androstenedione treatment (Figure 2C-D), suggesting that the protective effect of the SNP in the exemestane treated arm might be mainly due to slow proliferation caused by low *CYP19* expression in subjects carrying the variant SNP. While treatment with anastrozole in subjects carrying the variant SNP genotype upregulated *CSMD1* and *CYP19*, resulting in increased drug target for AIs. Therefore, we observed a more sensitive phenotype of anastrozole in LCLs containing the variant *CSMD1* rs6990851 SNP (Figure 3A). Therefore, the SNP was a protective SNP with outcomes in MA27, regardless of the

treatment arm, However, based on our results, the mechanisms underlying these association may be different between anastrozole and the other AIs.

The identification of anastrozole and SNP genotype-dependent regulation of gene expression (Figures 2B-G and 3) could be explained by a novel mechanism of anastrozole action, that is, anastrozole binds to ERα resulting in ERα degradation (18). At the transcriptional level, anastrozole-dependent transcripts significantly overlapped with E2, but also displayed significant differences from E2, indicating a unique function for anastrozole-ERα gene transcription regulation (Figure 4D). The differences between anastrozole and E2-driven transcriptional programs may be due to differential expression of co-regulators that dictate specific ERα-DNA binding and transcriptional activity. Like tamoxifen (34), it is also possible that anastrozole might exert different functions through ERα, either as an agonist or antagonist in a tissue context dependent manner, a process that is also dependent on the receptor-DNA complex interacting with different co-regulators (35). Additional work to decipher these hypotheses is ongoing.

Finally, the effect of anastrozole on ERα protein degradation is potentiated by E2 (Figure 4B). In a short-term randomized study, anastrozole treatment significantly reduced mean ER expression from baseline in breast cancer patients (36). The downregulation of cellular ERα protein occurred without a reduction in ESR1 mRNA, consistent with our findings. Taking advantage of this mechanism, we tested the combination of anastrozole + E2 as a potential therapeutic strategy, especially in AI- or fulvestrant-resistant breast cancer. We showed that anastrozole + E2 inhibits proliferation of AI- and fulvestrant-resistant breast cancer cells in addition to its effect in hormone therapy naïve breast cancer cells (Figures 5 and 6). Furthermore, the same results were also observed in breast cancer PDX derived organoids (Figure 5E-F). Hence, the combination might offer a potential alternative therapeutic strategy against refractory ER positive breast cancer. E2 is being used in the clinic to treat breast cancer with doses as high as 30mg/d (37). The E2 effect on tumor inhibition has also been observed in tamoxifen-resistant breast cancer in mice, where estrogen can reverse tamoxifen resistance (38). Therefore, the combination of anastrozole + E2 might be a feasible therapeutic option that could be tested in the future. In our study, we also showed that the combination of anastrozole and E2 was superior to E2 alone (Figure 5F), further suggesting that E2 potentiates the effect of anastrozole on ERα degradation. The development of CDK 4/6 inhibitors has changed the therapeutic management

of hormone receptor-positive (HR+) metastatic breast cancer (HR+ MBC). Palbociclib, ribociclib, and abemaciclib are approved in combination with an aromatase inhibitor or fulvestrant for HR+ MBC (39, 40). Abemaciclib is also approved as a monotherapy for pre-treated patients (41). Key questions in the field include whether all patients with HR+ MBC should receive a CDK 4/6 inhibitor up front and what is the mechanism of clinical resistance. Patients who progressed on CDK 4/6 inhibitor + AI are currently offered additional therapies such as fulvestrant as a single agent, but the PFS with fulvestrant in the post-CDK 4/6 setting is unclear. Therefore, there is a great need to identify additional therapies to improve outcome. Our observations here, combination of anastrozole and E2, may offer additional therapeutic strategies to further improve outcomes of HR+ MBC.

Taking advantage of the results of two GWAS with related but different phenotypes associated with AI action, we have identified a *CSMD1* SNP as a predicative marker for AI response. Furthermore, the cumulative effect of anastrozole + E2 on ERα degradation might provide an alternative therapy for ER-positive patients, especially those who are already resistant to hormonal therapy. The differences in E2 and anastrozole dependent transcription regulation should help us better understand mechanisms of anastrozole resistance, and could help identify additional drug targets or treatment options to overcome AI resistance.

Methods

GWAS of estrogen response in M3 cohort

For the genome-wide association analyses of estrogen suppression to anastrozole therapy, we used samples from the M3 AI Pharmacogenomics Study. To ensure that all included patients were compliant with therapy, we included only patients who had detectable levels of either anastrozole or one of its metabolites. Therefore, we excluded 12 patients who had a discordant change in direction between their estrone and estradiol concentrations after AI treatment. We also excluded 8 additional patients whose pre-anastrozole and on-anastrozole estradiol concentrations were either undetectable or zero. Our final analysis sample size was 624 patients. To assess SNP effects on estrogen response, three phenotypes were analyzed 1) absolute change in E1; 2) absolute change in E2; 3) absolute change in the sum of E1 and E2. A Van Der

Waerden transformation was applied to address the skewed Gaussian distributions. Linear regression models were used with additive SNP effects and the following covariates: age, BMI, the first 6 eigenvectors from a principal components analysis and either baseline E1, E2 or the sum of E1 and E2. QQ plots were used to assess adherence of the resultant p values to the null distribution. Common genes having SNPs reaching GWAS significance were retained for further analyses. All analyses were performed using R statistical computing software (v3.0.2) and Plink (v1.07) (7).

Survival analysis in the MA.27 cohort

To determine if the SNP was associated with breast cancer free interval (BCFI), the non-parametric log-rank test was initially performed with each SNP coded as a categorical variable as 0, 1, 2 copies of the minor allele. SNPs found to be associated with BCFI, were then forwarded to a Cox proportional hazards model where SNPs were modeled as a continuous dosage variable. In both cases, the null hypothesis of no association between SNP alleles and BCFI were being tested. Satisfaction of the assumption of proportional hazards was tested after fitting the Cox model in R (version 3.0.2) followed by the Grambsch and Therneau test. To select clinical variables that might confound the relationship between SNP and BCFI, univariate Cox regression models were fitted with drug usage, chemotherapy usage, tumor stage, age, BMI and PR status separately. For all continuous variables, the linearity assumption was tested and, if violated, that variable was modeled using restricted cubic splines. Variables found to have a significant association ($p<0.05$) with BCFI were included in a forward stepwise manner to build a multivariate Cox model with SNP. These analyses were performed in the full cohort, and also, separately within each treatment arm. To determine if the SNP modified the effect of the treatment on BCFI, Cox models were fitted with interaction terms between SNPs and treatment arm. Similarly, interactions between the SNPs and chemotherapy use, progesterone receptor status and tumor stage status were tested. All analyses were done in R (version 3.0.2).

We performed Exact Fisher tests to examine the imbalances between North American patients who were included in this GWAS and those who were not. Stepwise selection method was used to evaluate additional clinical variables associated with breast recurrence event. We employed a stratified genome-wide Cox-proportional hazards model using significant stratification factors with control for additional covariates including treatment arm, cohort, race, ER/PR status, T-

stage, ECOG performance score and bisphosphonate use. All the analyses were run using the R statistical computing package, PLINK, and SAS (SAS Institute, Cary, NC) (7).

RNA-Seq analysis and normalization

T47D cells were treated with vehicle, E2 (0.1 nM), anastrozole (10 nM), or a combination of E2 and anastrozole for 24 h. RNA-Seq was performed and analyzed as described in the Supplementary Methods. The RNAseq data is publicly available from NCBI Gene Expression Omnibus (http://www.ncbi.nlm.nih.gov/geo) under SuperSeries accession no. GSE150683.

Organoid derivation, 3D cell culture and viability assay

ER positive PDXs from the Breast Cancer Genome Guided Therapy Study (BEAUTY) were generated according to a previously described protocol (28). Tumors were injected subcutaneously into 6–8 week old female non-obese diabetic/severe combined immunodeficient NOD-SCID/IL2γ-receptor null (NSG) mice (Jackson Laboratories, Bar Harbor, Maine). Tumor cells from two breast cancer PDXs were isolated using the human Tumor Dissociation Kit (Miltenyi Biotec). Briefly, tumors were minced and then transferred into the gentle MACS C Tube and run through the 7C_h_TDK3 program according to manufacturer's protocol. The tubes were then centrifuged to collect the sample material. Samples were resuspended and applied to a MACS SmartStrainer (70 μm). A Mouse Cell Depletion Kit (Miltenyi Biotec) was used to enrich human cells. Specifically, the cell pellet was suspended in buffer, 20μL of the Mouse Cell Depletion Cocktail was added and the mixtures were incubated for 15 minutes at 4 °C. Then magnetic separation with LS Columns was performed to collect human cells. Organoids were cultured in 96-well low binding NanoCulture plate (Organogenix) in DMEM supplemented with 10% FCS, 1% glutamax, 1% sodium pyruvate, non-essential amino acids, and 1% Penicillin-Streptomycin (Life Technologies) at 37°C, 5% CO_2. Details of the organoid viability assay are described in the Supplementary Methods.

Statistical analysis

For cell survival, cell proliferation, gene expression, and quantifications, data are represented as the mean ± SEM of three independent experiments. Unless otherwise described, 2-way ANOVA (Analysis of Variance) was performed to test group difference. Then post-hoc analysis was

carried out to check if specific groups are significantly different or similar. Tukey HSD (Tukey Honest Significant Differences, R function: TukeyHSD()), which is essentially a modified t-test corrected for multiple comparisons, was applied in this analysis. Statistical significance level is 0.05.

Study approval

M3 study was reviewed and approved by local institutional review boards at all participating institutions. Written informed consent was obtained from each patient. MA.27 study was approved by local institutional review boards in accordance with assurances filed with, and approved by, the Department of Health and Human Services. All animal studies were reviewed and approved by the Mayo Clinic Institutional Animal Care and Use Committee.

Author contributions

Conception and design: J. Cairns, J.N. Ingle, L. Wang.

Development of methodology: J. Cairns, T. Dudenkov, L. Wang, J.N. Ingle, R.M. Weinshilboum.

Acquisition of data: J. Cairns, J.N. Ingle, A.U. Buzdar, M.E. Robson, M.J. Ellis, P.E. Goss, L.E. Shepherd, M.P. Goetz, B. Goodnature.

Analysis and interpretation of data (e.g., statistical analysis, biostatistics, computational analysis): J. Cairns, T. Dudenkov, K.R. Kalari, E.E. Carlson, J. Na, H. Li, M. Ghanat Bari.

Writing, review, and/or revision of the manuscript: J. Cairns, J.N. Ingle, L. Wang, T. Dudenkov.

Administrative, technical, or material support (i.e., reporting or organizing data, constructing databases): J. Cairns, T. Dudenkov, E.E. Carlson, M. Ghanat Bari.

Study supervision: J. Cairns, J.N. Ingle, L. Wang, R.M. Weinshilboum.

Acknowledgments

The authors acknowledge the women who participated in the M3 and MA.27 clinical trials and provided DNA and consent for its use in genetic studies. This research was supported by the Breast Cancer Research Foundation (BCRF), UG1CA18967, P50CA116201 (Mayo Clinic Breast Cancer Specialized Program of Research Excellence), U1961388 (the Pharmacogenomics Research Network), the George M. Eisenberg Foundation for Charities, the Nan Sawyer Breast Cancer Fund, and NIH/NCI Cancer Center Support Grant P30 CA008748.

References

1. Early Breast Cancer Trialists' Collaborative G, Davies C, Godwin J, Gray R, Clarke M, Cutter D, et al. Relevance of breast cancer hormone receptors and other factors to the efficacy of adjuvant tamoxifen: patient-level meta-analysis of randomised trials. *Lancet.* 2011;378(9793):771-84.
2. Early Breast Cancer Trialists' Collaborative G. Aromatase inhibitors versus tamoxifen in early breast cancer: patient-level meta-analysis of the randomised trials. *Lancet.* 2015;386(10001):1341-52.
3. Mauri D, Pavlidis N, Polyzos NP, and Ioannidis JP. Survival with aromatase inhibitors and inactivators versus standard hormonal therapy in advanced breast cancer: meta-analysis. *J Natl Cancer Inst.* 2006;98(18):1285-91.
4. Benz CC, Scott GK, Sarup JC, Johnson RM, Tripathy D, Coronado E, et al. Estrogen-dependent, tamoxifen-resistant tumorigenic growth of MCF-7 cells transfected with HER2/neu. *Breast Cancer Res Treat.* 1992;24(2):85-95.
5. Massarweh S, Osborne CK, Jiang S, Wakeling AE, Rimawi M, Mohsin SK, et al. Mechanisms of tumor regression and resistance to estrogen deprivation and fulvestrant in a model of estrogen receptor-positive, HER-2/neu-positive breast cancer. *Cancer Res.* 2006;66(16):8266-73.
6. Middlebrooks CD, Banday AR, Matsuda K, Udquim KI, Onabajo OO, Paquin A, et al. Association of germline variants in the APOBEC3 region with cancer risk and enrichment with APOBEC-signature mutations in tumors. *Nat Genet.* 2016;48(11):1330-8.

7. Ingle JN, Xie F, Ellis MJ, Goss PE, Shepherd LE, Chapman JW, et al. Genetic Polymorphisms in the Long Noncoding RNA MIR2052HG Offer a Pharmacogenomic Basis for the Response of Breast Cancer Patients to Aromatase Inhibitor Therapy. *Cancer Res.* 2016;76(23):7012-23.
8. Ma CX, Reinert T, Chmielewska I, and Ellis MJ. Mechanisms of aromatase inhibitor resistance. *Nat Rev Cancer.* 2015;15(5):261-75.
9. Li S, Shen D, Shao J, Crowder R, Liu W, Prat A, et al. Endocrine-therapy-resistant ESR1 variants revealed by genomic characterization of breast-cancer-derived xenografts. *Cell Rep.* 2013;4(6):1116-30.
10. Aguilar H, Sole X, Bonifaci N, Serra-Musach J, Islam A, Lopez-Bigas N, et al. Biological reprogramming in acquired resistance to endocrine therapy of breast cancer. *Oncogene.* 2010;29(45):6071-83.
11. Zilli M, Grassadonia A, Tinari N, Di Giacobbe A, Gildetti S, Giampietro J, et al. Molecular mechanisms of endocrine resistance and their implication in the therapy of breast cancer. *Biochim Biophys Acta.* 2009;1795(1):62-81.
12. Wang L, Ellsworth KA, Moon I, Pelleymounter LL, Eckloff BW, Martin YN, et al. Functional genetic polymorphisms in the aromatase gene CYP19 vary the response of breast cancer patients to neoadjuvant therapy with aromatase inhibitors. *Cancer Res.* 2010;70(1):319-28.
13. Smith IE, and Dowsett M. Aromatase inhibitors in breast cancer. *N Engl J Med.* 2003;348(24):2431-42.
14. Sendur MA, Aksoy S, Zengin N, and Altundag K. Efficacy of adjuvant aromatase inhibitor in hormone receptor-positive postmenopausal breast cancer patients according to the body mass index. *Br J Cancer.* 2012;107(11):1815-9.
15. Pfeiler G, Konigsberg R, Fesl C, Mlineritsch B, Stoeger H, Singer CF, et al. Impact of body mass index on the efficacy of endocrine therapy in premenopausal patients with breast cancer: an analysis of the prospective ABCSG-12 trial. *J Clin Oncol.* 2011;29(19):2653-9.
16. Goss PE, Ingle JN, Pritchard KI, Ellis MJ, Sledge GW, Budd GT, et al. Exemestane versus anastrozole in postmenopausal women with early breast cancer: NCIC CTG MA.27--a randomized controlled phase III trial. *J Clin Oncol.* 2013;31(11):1398-404.

17. Smith I, Yardley D, Burris H, De Boer R, Amadori D, McIntyre K, et al. Comparative Efficacy and Safety of Adjuvant Letrozole Versus Anastrozole in Postmenopausal Patients With Hormone Receptor-Positive, Node-Positive Early Breast Cancer: Final Results of the Randomized Phase III Femara Versus Anastrozole Clinical Evaluation (FACE) Trial. *J Clin Oncol.* 2017;35(10):1041-8.
18. Ingle JN CJ, Suman VJ, Shepherd LE, Fasching PA, Hoskin TL, Singh RJ, Desta Z, Kalari KR, Ellis MJ, Goss PE, Chen BE, Volz B, Barman P, Carlson EE, Haddad T, Goetz MP, Goodnature B, Cuellar ME, Walters MA, Correia C, Kaufmann SH, Weinshilboum RM, Wang L. Anastrozole has an association between degree of estrogen suppression and outcomes in early breast cancer and is a ligand for estrogen receptor α. *Clin Cancer Res.* 2020; Epub 2/27/2020.
19. Ingle JN, Kalari KR, Buzdar AU, Robson ME, Goetz MP, Desta Z, et al. Estrogens and their precursors in postmenopausal women with early breast cancer receiving anastrozole. *Steroids.* 2015;99(Pt A):32-8.
20. Ingle JN, Liu M, Wickerham DL, Schaid DJ, Wang L, Mushiroda T, et al. Selective estrogen receptor modulators and pharmacogenomic variation in ZNF423 regulation of BRCA1 expression: individualized breast cancer prevention. *Cancer Discov.* 2013;3(7):812-25.
21. Cairns J, Ingle JN, Kalari KR, Shepherd LE, Kubo M, Goetz MP, et al. The lncRNA MIR2052HG regulates ERalpha levels and aromatase inhibitor resistance through LMTK3 by recruiting EGR1. *Breast Cancer Res.* 2019;21(1):47.
22. Macedo LF, Sabnis G, and Brodie A. Aromatase inhibitors and breast cancer. *Ann N Y Acad Sci.* 2009;1155:162-73.
23. Neven P. The origin of postmenopausal oestrogens. *Eur J Cancer.* 2002;38 Suppl 6:S29-30.
24. Tang MR, Wang YX, Guo S, Han SY, and Wang D. CSMD1 exhibits antitumor activity in A375 melanoma cells through activation of the Smad pathway. *Apoptosis.* 2012;17(9):927-37.
25. Liang N, Xu Y, Yin Y, Yao G, Tian H, Wang G, et al. Steroidogenic factor-1 is required for TGF-beta3-mediated 17beta-estradiol synthesis in mouse ovarian granulosa cells. *Endocrinology.* 2011;152(8):3213-25.

26. Powers GL, Ellison-Zelski SJ, Casa AJ, Lee AV, and Alarid ET. Proteasome inhibition represses ERalpha gene expression in ER+ cells: a new link between proteasome activity and estrogen signaling in breast cancer. *Oncogene.* 2010;29(10):1509-18.
27. Thewes V, Simon R, Hlevnjak M, Schlotter M, Schroeter P, Schmidt K, et al. The branched-chain amino acid transaminase 1 sustains growth of antiestrogen-resistant and ERalpha-negative breast cancer. *Oncogene.* 2017;36(29):4124-34.
28. Goetz MP, Kalari KR, Suman VJ, Moyer AM, Yu J, Visscher DW, et al. Tumor Sequencing and Patient-Derived Xenografts in the Neoadjuvant Treatment of Breast Cancer. *J Natl Cancer Inst.* 2017;109(7).
29. Nardone A, De Angelis C, Trivedi MV, Osborne CK, and Schiff R. The changing role of ER in endocrine resistance. *Breast.* 2015;24 Suppl 2:S60-6.
30. Robertson JFR, Bondarenko IM, Trishkina E, Dvorkin M, Panasci L, Manikhas A, et al. Fulvestrant 500 mg versus anastrozole 1 mg for hormone receptor-positive advanced breast cancer (FALCON): an international, randomised, double-blind, phase 3 trial. *Lancet.* 2016;388(10063):2997-3005.
31. Lerebours F, Rivera S, Mouret-Reynier MA, Alran S, Venat-Bouvet L, Kerbrat P, et al. Randomized phase 2 neoadjuvant trial evaluating anastrozole and fulvestrant efficacy for postmenopausal, estrogen receptor-positive, human epidermal growth factor receptor 2-negative breast cancer patients: Results of the UNICANCER CARMINA 02 French trial (UCBG 0609). *Cancer.* 2016;122(19):3032-40.
32. Edavana VK, Dhakal IB, Williams S, Penney R, Boysen G, Yao-Borengasser A, et al. Potential role of UGT1A4 promoter SNPs in anastrozole pharmacogenomics. *Drug Metab Dispos.* 2013;41(4):870-7.
33. Gordan R, Shen N, Dror I, Zhou T, Horton J, Rohs R, et al. Genomic regions flanking E-box binding sites influence DNA binding specificity of bHLH transcription factors through DNA shape. *Cell Rep.* 2013;3(4):1093-104.
34. Zhang H, McElrath T, Tong W, and Pollard JW. The molecular basis of tamoxifen induction of mouse uterine epithelial cell proliferation. *J Endocrinol.* 2005;184(1):129-40.
35. Shanle EK, and Xu W. Endocrine disrupting chemicals targeting estrogen receptor signaling: identification and mechanisms of action. *Chem Res Toxicol.* 2011;24(1):6-19.

36. Robertson JF, Dixon JM, Sibbering DM, Jahan A, Ellis IO, Channon E, et al. A randomized trial to assess the biological activity of short-term (pre-surgical) fulvestrant 500 mg plus anastrozole versus fulvestrant 500 mg alone or anastrozole alone on primary breast cancer. *Breast Cancer Res.* 2013;15(2):R18.
37. Ellis MJ, Gao F, Dehdashti F, Jeffe DB, Marcom PK, Carey LA, et al. Lower-dose vs high-dose oral estradiol therapy of hormone receptor-positive, aromatase inhibitor-resistant advanced breast cancer: a phase 2 randomized study. *JAMA.* 2009;302(7):774-80.
38. Osipo C, Gajdos C, Cheng D, and Jordan VC. Reversal of tamoxifen resistant breast cancer by low dose estrogen therapy. *J Steroid Biochem Mol Biol.* 2005;93(2-5):249-56.
39. Litwin MS, and First RA. Maculoerythematous rash after lumbar sympathectomy. *N Engl J Med.* 1961;265:484-6.
40. Goetz MP, Toi M, Campone M, Sohn J, Paluch-Shimon S, Huober J, et al. MONARCH 3: Abemaciclib As Initial Therapy for Advanced Breast Cancer. *J Clin Oncol.* 2017;35(32):3638-46.
41. Dickler MN, Tolaney SM, Rugo HS, Cortes J, Dieras V, Patt D, et al. MONARCH 1, A Phase II Study of Abemaciclib, a CDK4 and CDK6 Inhibitor, as a Single Agent, in Patients with Refractory HR(+)/HER2(-) Metastatic Breast Cancer. *Clin Cancer Res.* 2017;23(17):5218-24.

Figures and figure legends

Figure 1. Discovery of *CSMD1* SNPs. (**A**) Manhattan plot of M3 GWAS results for change in estradiol upon anastrozole treatment. (**B**) Genomic position of *CSMD1* SNP associated with BCFI in MA.27. (**C**) Kaplan-Meier plots of time to breast events in MA.27 for different copies of *CSMD1* variant allele rs6990851. P value represents stratified Cox-proportional hazards analysis.

Figure 1

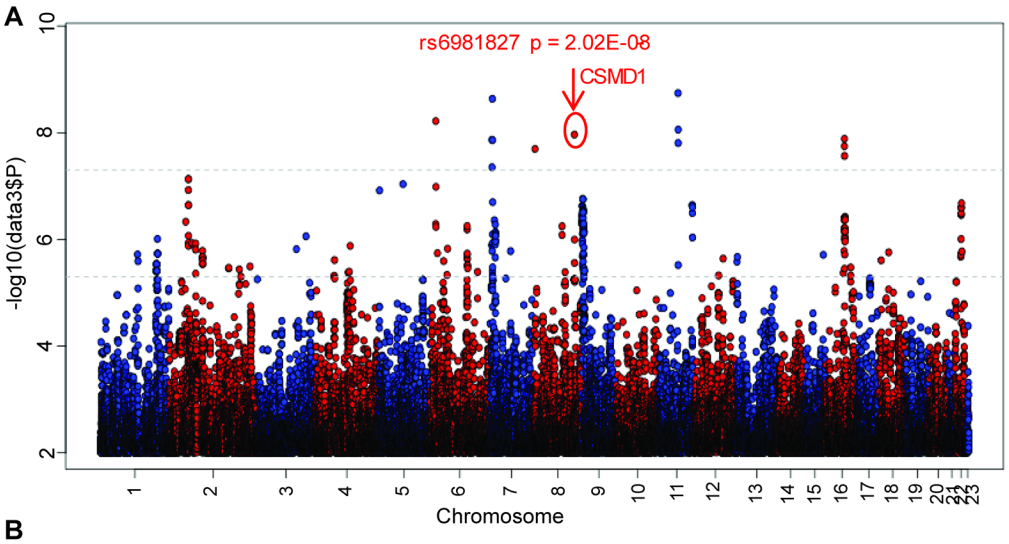
A
rs6981827 p = 2.02E-08
CSMD1
-log10(data3$P)
Chromosome

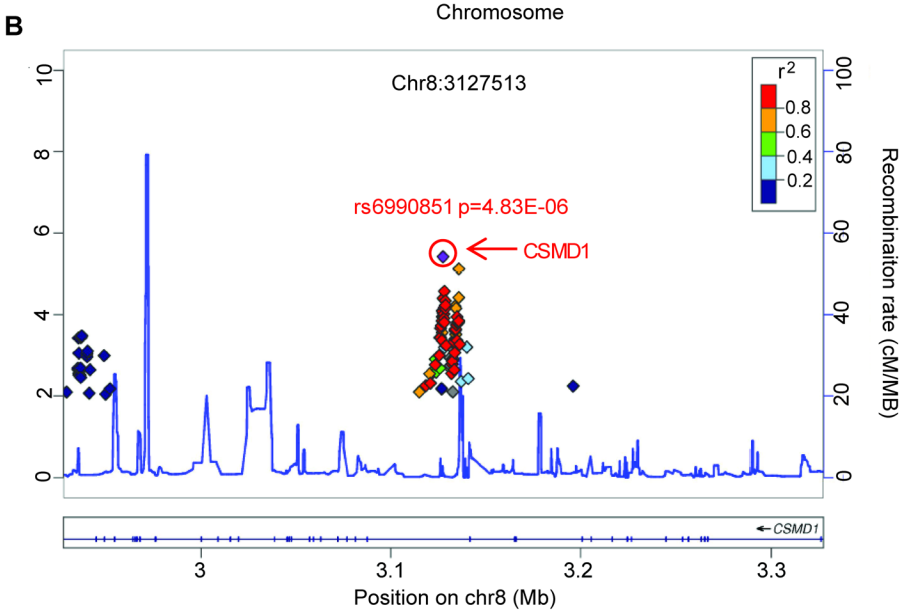
B
Chr8:3127513
r2
0.8
0.6
0.4
0.2
rs6990851 p=4.83E-06
CSMD1
Recombinaiton rate (cM/MB)
CSMD1
Position on chr8 (Mb)

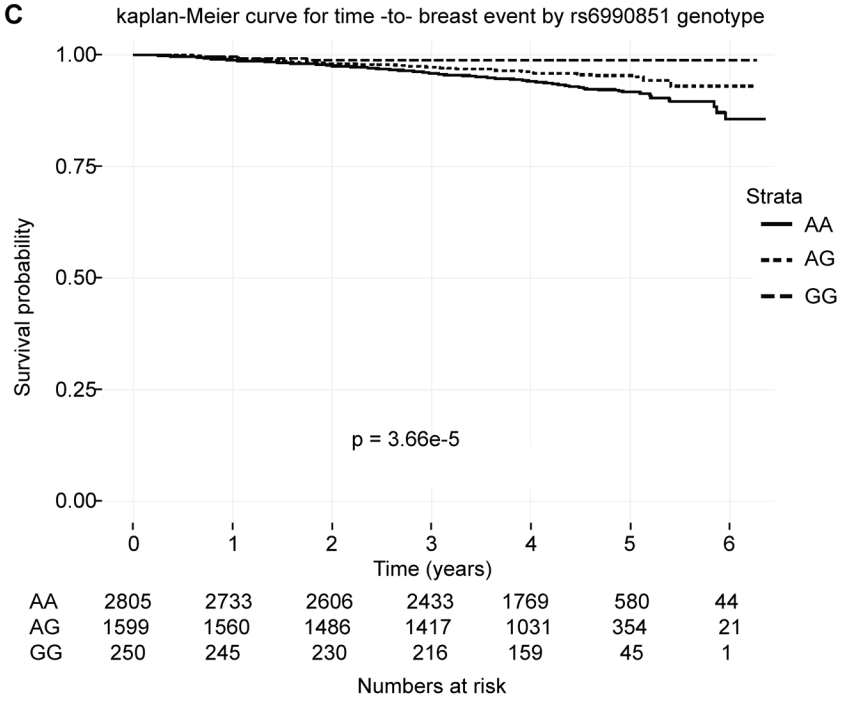
C
kaplan-Meier curve for time -to- breast event by rs6990851 genotype
Survival probability
Strata
AA
AG
GG
p = 3.66e-5
Time (years)
AA 2805 2733 2606 2433 1769 580 44
AG 1599 1560 1486 1417 1031 354 21
GG 250 245 230 216 159 45 1
Numbers at risk

Figure 2. *CSMD1* SNP-androstenedione- and anastrozole -dependent regulation of *CSMD1* and *CYP19A1* expression. (**A**) *CYP19A1* mRNA expression levels in *CSMD1* overexpressed breast cancer cells and human adipocytes. (**B-E**) SNP-dependent gene regulation of *CSMD1* and *CYP19A1* expression in the presence of increasing concentrations of androstenedione (A) or 20 nM androstenedione plus increasing concentrations of AIs (Anastrozole: Ana; letrozole: Let; Exemestane: Exe) in lymphoblastoid cell lines (LCLs) selected based on the rs6990851 SNP genotype. *CSMD1* WT: homozygous WT LCLs (n=5), *CSMD1* V: homozygous variant LCLs (n=5). (**F**) Schematic figure shows the EREs surrounding the rs6990851SNP. Primers 1 and 2 were used in the ChIP assays to determine the regions around the two EREs. (**G**) ERα ChIP assay shows SNP dependent ERα binding to the ERE region that is 296 bp upstream from the rs6990851 SNP in LCLs with different genotypes treated with the indicated drugs. Error bars (**A, B-D, G**) represent SEM of three independent experiments. *$p < 0.05$; ** $p< 0.01$. Statistical test: 2-way ANOVA.

Figure 2

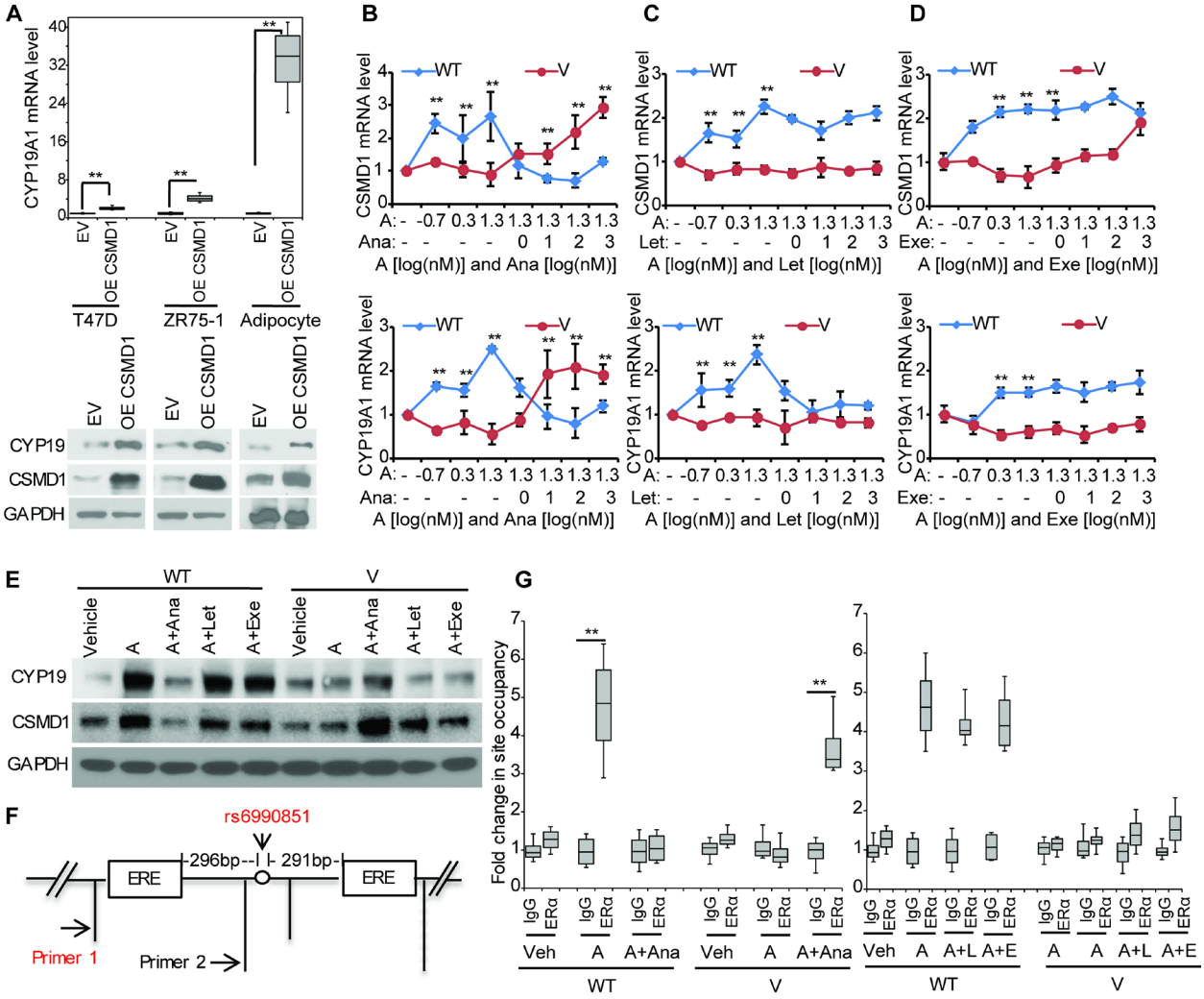
A
CYP19A1 mRNA level
EV
OE CSMD1
T47D
ZR75-1
Adipocyte
CYP19
CSMD1
GAPDH
B
C
D
CSMD1 mRNA level
CYP19A1 mRNA level
WT
V
A: - -0.7 0.3 1.3 1.3 1.3 1.3 1.3
Ana: - - - - 0 1 2 3
Let: - - - - 0 1 2 3
Exe: - - - - 0 1 2 3
A [log(nM)] and Ana [log(nM)]
A [log(nM)] and Let [log(nM)]
A [log(nM)] and Exe [log(nM)]
E
Vehicle
A
A+Ana
A+Let
A+Exe
F
rs6990851
296bp
291bp
ERE
Primer 1
Primer 2
G
Fold change in site occupancy
IgG
ERα
Veh
A+L
A+E

Figure 3. Effects of *CSMD1* SNP on anastrozole response and mechanisms involved in *CSMD1* regulation of *CYP19*. (**A**) *CSMD1* SNP- dependent effect on AI responses. w/w: homozygous WT (n=5), w/v: heterozygous (n=5) and v/v: homozygous variant LCLs (n=5). (w/w vs w/v: $p < 0.0001$; w/w vs v/v: $p < 0.0001$). (**B**) Increased anastrozole sensitivity in cells overexpressing *CSMD1* (Empty vector (EV):Ana vs OE CSMD1-Ana: $p < 0.0001$). Side panel shows mRNA expression in cell lines tested. MCF7AC1 (AC1), AC1-LetR (LetR), and Adipocyte. (**C)** Western blot showing CYP19A1 expression in three single clones of *CYP19A1* knockout T47D cells using CRISPR/Cas9. KO-3 was selected for further experiments. (**D**) Anastrozole sensitivity after overexpressing CSMD1 in *CYP19A1* knockout T47D cells (KO) and control cells (Con) shows the reversal of anastrozole sensitivity caused by overexpression of CSMD1. (**E**) Detection of CSMD1 and SMAD3 interaction using immunoprecipitation, followed by Western blot analysis with indicated antibodies. (**F**) Increased SMAD3-TGFβR binding in CSMD1 overexpressed cells. (**G**) *CSMD1* SNP effect on pSMAD3 and CYP19A1 protein levels. A; androstenedione, Ana: anastrozole, Let: letrozole and Exe: exemestane. Error bars represent the SEM of three independent experiments. *$p < 0.05$; ** $p < 0.01$. Statistical test: 2-way ANOVA plus Tukey.

Figure 3

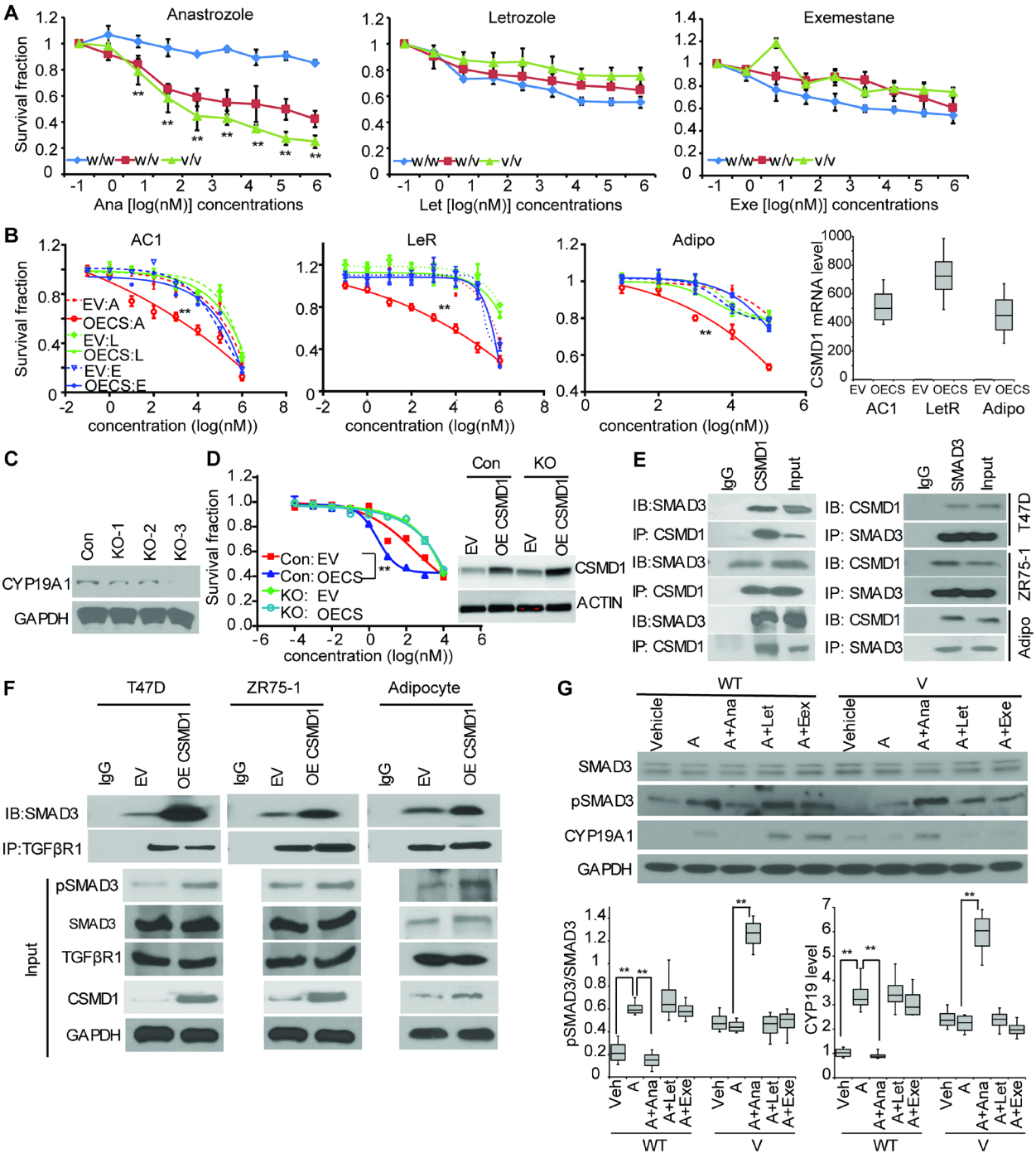
A
Anastrozole
Letrozole
Exemestane
Survival fraction
w/w w/v v/v
Ana [log(nM)] concentrations
Let [log(nM)] concentrations
Exe [log(nM)] concentrations
B
AC1
LeR
Adipo
EV:A
OECS:A
EV:L
OECS:L
EV:E
OECS:E
concentration (log(nM))
CSMD1 mRNA level
EV OECS EV OECS EV OECS
AC1 LetR Adipo
C
Con KO-1 KO-2 KO-3
CYP19A1
GAPDH
D
Con KO
EV OE CSMD1 EV OE CSMD1
Con: EV
Con: OECS
KO: EV
KO: OECS
CSMD1
ACTIN
E
IgG CSMD1 Input
IB:SMAD3
IP: CSMD1
IB: CSMD1
IP: SMAD3
IgG SMAD3 Input
T47D
ZR75-1
Adipo
F
T47D
ZR75-1
Adipocyte
IgG EV OE CSMD1
IB:SMAD3
IP:TGFβR1
Input
pSMAD3
SMAD3
TGFβR1
CSMD1
GAPDH
G
WT
V
Vehicle A A+Ana A+Let A+Exe
SMAD3
pSMAD3
CYP19A1
GAPDH
pSMAD3/SMAD3
CYP19 level
Veh A A+Ana A+Let A+Exe
WT V

Figure 4. Anastrozole potentiates estrogen effect on ERα transcription activity and ERα degradation. (**A**) ERE dependent-Luciferase assay in *CYP19A1* CRISPR KO T47D cells treated with indicated concentrations of E2, anastrozole (Ana), letrozole (Let) or exemestane (Exe). (**B**) Cells treated with E2 and anastrozole either alone or combined at the indicated concentrations. Western blot was performed to determine ERα protein level. (**C**) Anastrozole induced ERα degradation is proteasome dependent. Cells treated with vehicle, 100 nM anastrozole or anastrozole plus 20 μM 3MA or 10 μM MG132 following western blot analysis of ERα protein levels. (**D**) Venn diagram showing the overlap between genes differentially expressed in response to anastrozole with or without E2 (FDR <0.05). Error bars represent the SEM of three independent experiments. *p < 0.05; ** p<0.01. Statistical test: 1-tailed t-test, bonferroni correction for multiple testing.

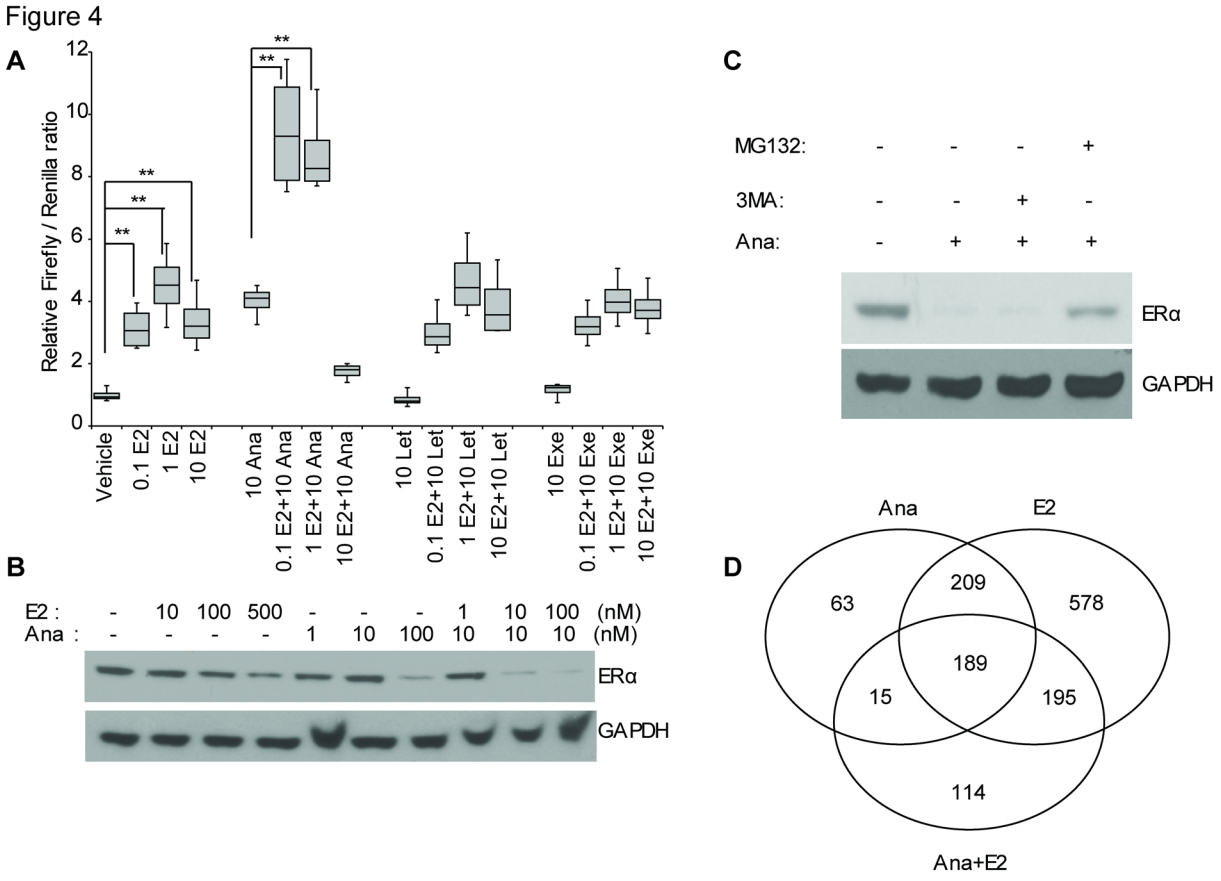

Figure 5. Sensitization effect of E2 on anastrozole response. (**A-C**) Dose response of anastrozole in the presence of E2 at indicated concentrations in CYP19A1 KO cells (**A**), (Ana vs Ana +10E2: $p<0.0001$; Ana vs Ana +100E2: $p<0.0001$); AC1-LetR cells, the letrozole resistant cells (**B**), (Ana vs Ana +10E2: $p<0.0001$; Ana vs Ana +100E2: $p<0.0001$); and MCF7/Ana^{R}, the anastrozole resistant cells (**C**), (Ana vs Ana +10E2: $p<0.0001$; Ana vs Ana +100E2: $p<0.0001$). (**D**) Western blot and quantification of ERα protein levels after anastrozole and E2 treatment. Error bars represent the SEM of three independent experiments. *$p < 0.05$; ** $p<0.01$. Statistical test: 2-way ANOVA plus Tukey.

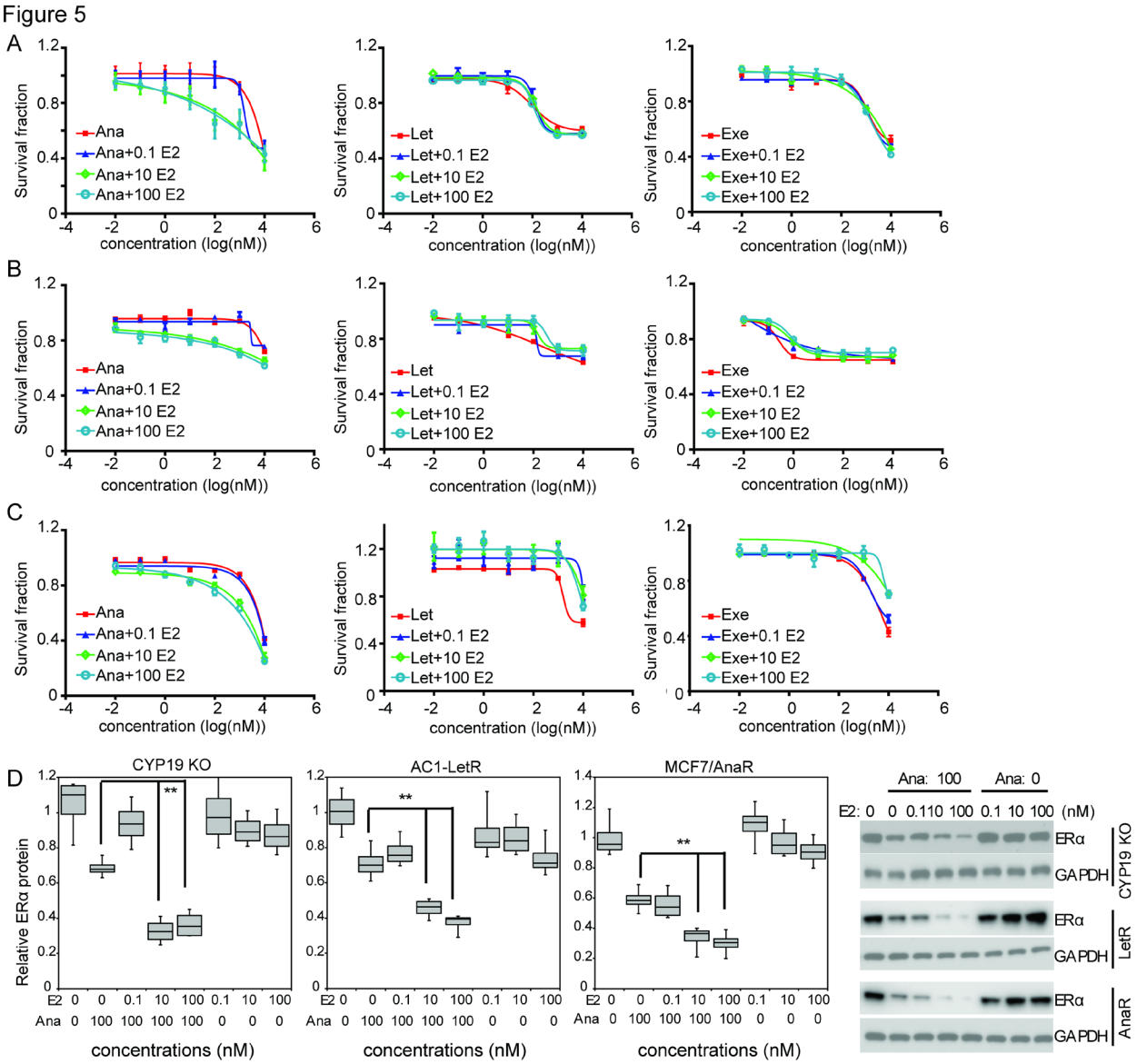

Figure 6. Sensitization effect of E2 on anastrozole response in breast cancer PDX derived organoids. (**A**) AI dose response in the presence of E2 in three organoids derived from breast cancer patients. Western blot showed ER positivity in the organoids. (ER positive control: MCF7 and BT474; ER negative control: MDA-231). (**B**) Organoid growth curves in the presence of 200nM anastrozole and/or 100nM E2. Error bars represent the SEM of three independent experiments. *p < 0.05; **p<0.01. Statistical test: 2-way ANOVA plus Tukey.

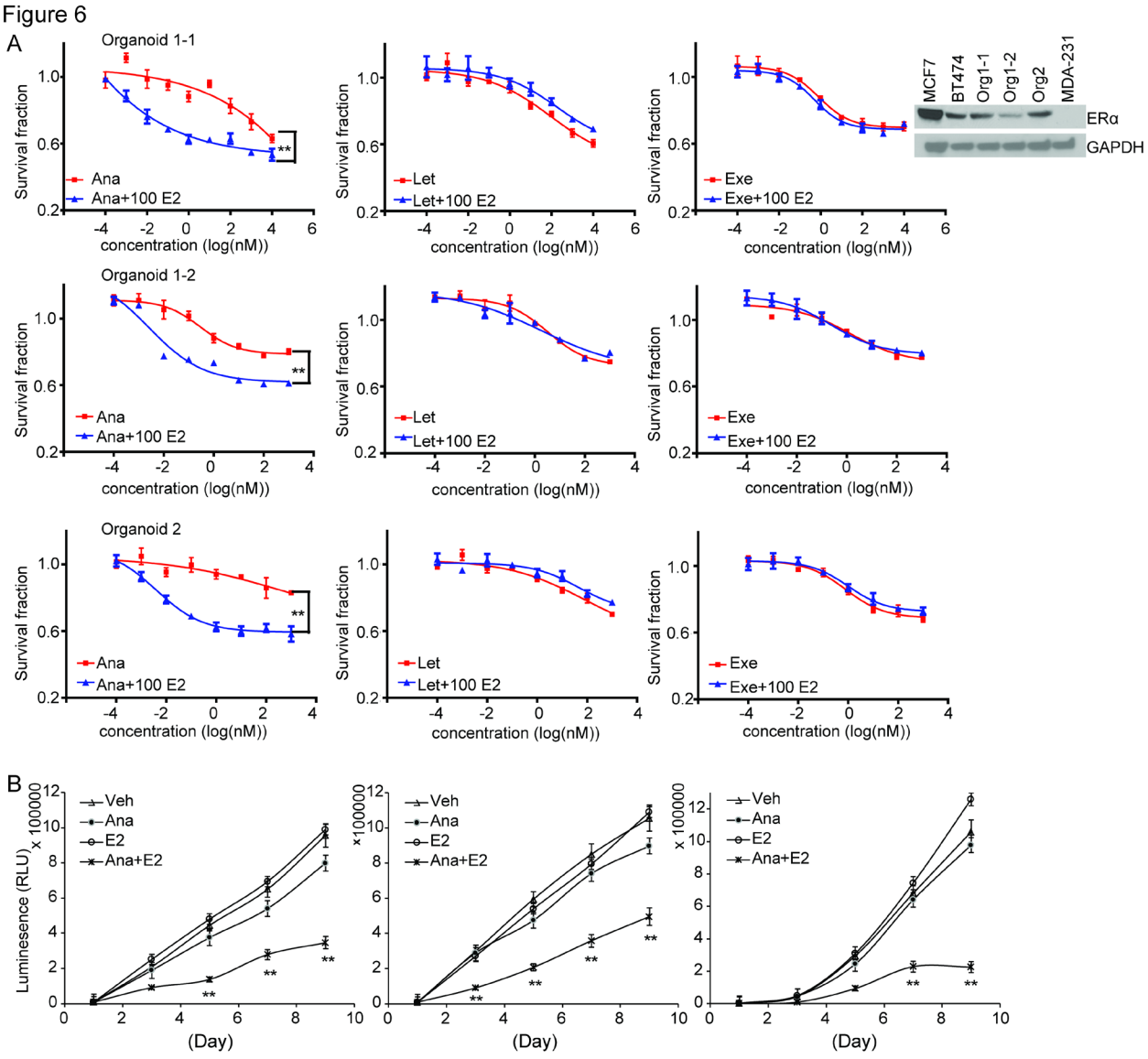

Figure 7. The comparison of efficacy between anastrozole plus E2 versus fulvestrant. (**A**) Effects of anastrozole + E2 in fulvestrant resistant cells. Fulvestrant (F) vs Ana: p=0.0009; F vs Ana+10E2: p<0.0001; F vs Ana+100E2: p<0.0001; F vs Ana+500E2: p<0.0001; Ana vs Ana+10E2: p=0.0288; Ana vs Ana+100E2: p<0.0001; Ana vs Ana+500E2: p<0.0001. Quantitative analysis of survival cells corrected back to vehicle treatment was performed after 3 days of treatment with indicated drugs, as shown in the bar graph. *p < 0.05; **p<0.01. Statistical test: 2-way ANOVA plus Tukey. (**B-C**) Comparison of anastrozole + E2 with fulvestrant in anastrozole-resistant MCF7/AnaR and three AI-naïve cell lines (**B**), as well as in PDX derived organoids (**C**). Quantitative analysis of survival cells corrected back to vehicle treatment was performed, as shown in the bar graph 3 days after treatment. Error bars represent the SEM of three independent experiments. MCF7/AnaR: F vs Ana: p<0.0001; F vs Ana+100E2: p=0.2093; Ana vs Ana+100E2: p <0.0001. MCF7AC1: F vs Ana+100E2: p<0.0001; Ana vs Ana+100E2: p=0.0013. ZR-75-1: F vs Ana+100E2: p<0.0001; Ana vs Ana+100E2: p<0.0001. T47D: F vs Ana+100E2: p<0.0001; Ana vs Ana+100E2: p<0.0001. Organoid-1-1: F vs Ana+100E2: p<0.0001; Ana vs Ana+100E2: p=0.0002; Ana vs F: p=0.02. Organoid-1-2: F vs Ana+100E2: p=0.0013; Ana vs Ana+100E2: p<0.0001; Ana vs F: p=0.013. Organoid-2: F vs Ana+100E2: p<0.0001; Ana vs Ana+100E2: p=0.0002; Ana vs F: p=0.0026. *p < 0.05; **p<0.01. Statistical test: 2-way ANOVA plus Tukey.

Figure 7

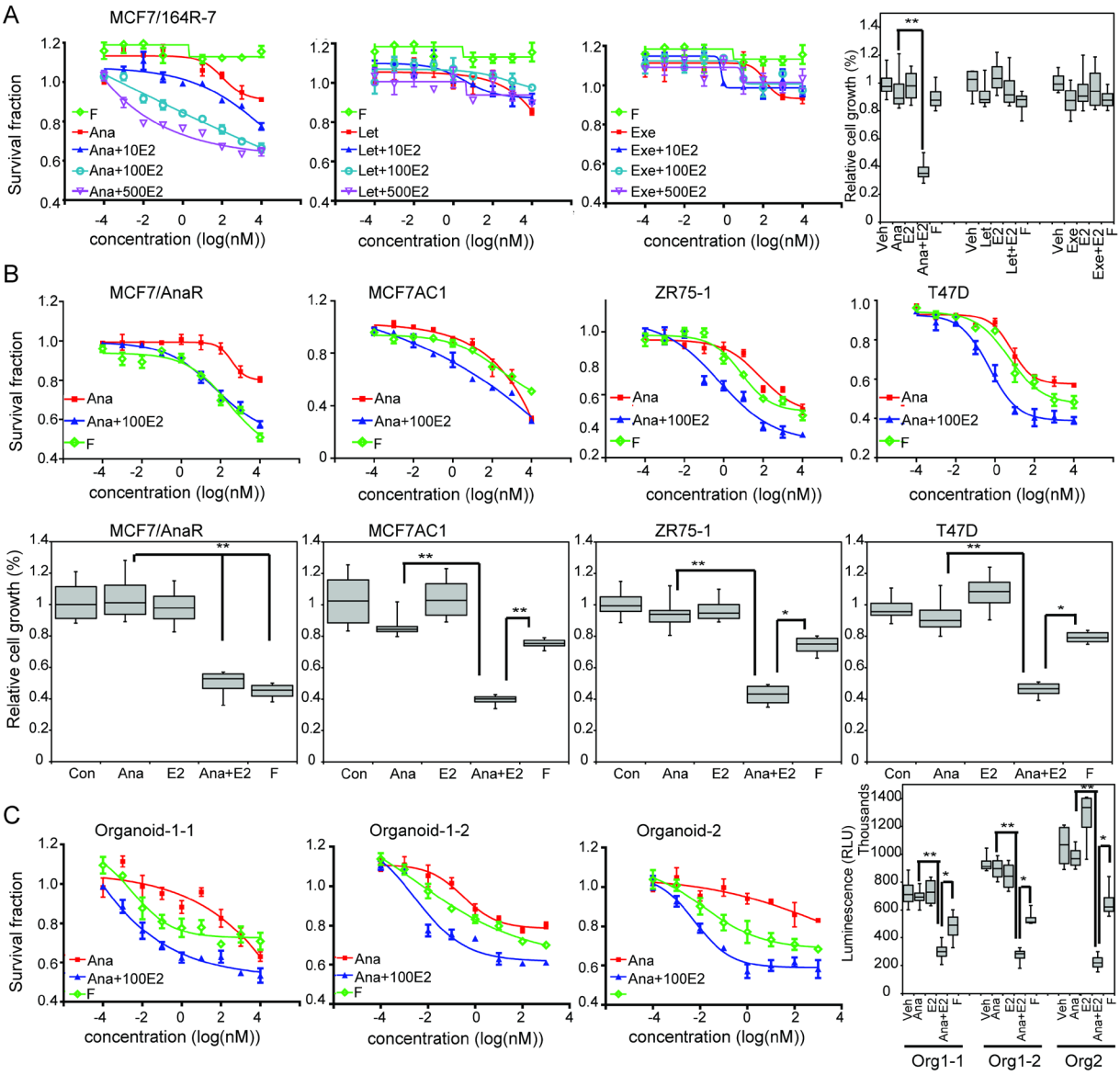
A
MCF7/164R-7
Survival fraction
concentration (log(nM))
F
Ana
Ana+10E2
Ana+100E2
Ana+500E2
Let
Let+10E2
Let+100E2
Let+500E2
Exe
Exe+10E2
Exe+100E2
Exe+500E2
Relative cell growth (%)
Veh
Ana
E2
Ana+E2
F
Let
Let+E2
Exe
Exe+E2
B
MCF7/AnaR
MCF7AC1
ZR75-1
T47D
Con
C
Organoid-1-1
Organoid-1-2
Organoid-2
Luminescence (RLU)
Thousands
Org1-1
Org1-2
Org2